

Mechanical Properties of Al/PU/Perforated CU/PU/Al Sandwich Composites

Saeed Mousa^{a*}, Hossam El-Din M. Sallam^b, Amr A. Abd-Elhady^{c*}

^aJazan University, Faculty of Engineering, 706, Jazan, Kingdom of Saudi Arabia

^bZagazig University, Department of Materials Engineering, 44519, Zagazig, Egypt

^cHelwan University, Department of Mechanical Design, Mataria, 11718, Cairo, Egypt

Received: February 28, 2021; Revised: May 21, 2021; Accepted: June 04, 2021

In the present work, the warm roll bonding (WRB) technique was adopted to fabricate 3 layers of Aluminum-perforated Copper 260-Aluminum (AL/perforated CU/AL), and five layers of (AL/Polyurethane (PU)/perforated CU/PU/AL) sandwich composites. Two different tests were adopted, namely peel test and small punch test (SPT), to study the peel strength and flexural behavior of these sandwich composites, respectively. The main manufacturing parameters, including interface properties, rolling speed, and the number of passes, which control the strength and integrity of these sandwich composites were studied experimentally. Furthermore, the three-dimensional finite element method was carried out to study the effect of the presence of pre-crack on the peeling test and SPT specimens numerically. The present results indicated that the peeling resistance is mainly dependent on the roughness of the interface and elapsed time in manufacturing processes. The flexural behavior of sandwich composites measured from SPT agrees with the first principles of mechanics of materials, i.e. there is a marginal effect of the bond strength between the layers.

Keywords: Warm roll bonding, aluminum sandwich composites, Small Punch Test specimens, peel test, cracked specimens.

1. Introduction

To achieve superior properties, for instance, lightweight properties, good thermal conductivity, anti-corrosion properties, wear resistance, and so forth, the multilayer composites were innovated for these reasons. Multilayer composites can be used in many applications such as automobile and marine industries. Multilayer composites showed synergistic behavior, i.e. preserve the original properties of the constituent materials in addition to give extra characteristics¹⁻⁴. For example but not limited to, metal/polymer/metal composites are used in lightweight applications with a high specific strength. AL/CU multilayer composites are incorporated in the thermal conductivity products³.

Several processes can be used to produce such composites, such as explosive bonding, adhesive bonding, or roll bonding (cold, warm, and hot). The roll bonding process is the most economical and productive manufacturing process that can be used to fabricate the multilayer composites⁴. In general, two or more strips (metal or polymer) are stacked together and pass through a pair of rolls. After proper deformation, a solid-state joining between the original individual material strips will be produced. Before roll bonding, the surface must be prepared and cleaned^{5,6}. Soltan Ali Nezhad et al.⁷ studied the joint quality of aluminum and low carbon steel strips produced by warm rolling. Metal-polymer-metal multilayer composites produced using warm roll bonding (WRB) process and without any adhesive between the layers (direct adhesion)⁸⁻¹⁰. Al5754 alloys were produced in multilayers

ways using cold roll bonding¹¹. Rolling can be conducted at room temperature or elevated temperatures. In WRB, the addition of energy provided by the preheating of the sheets aids the kinetics of welding⁴. Cleaning and roughening the interface are important factors to enhance the integrity of sandwich composites¹².

To get superior bonding properties in WRB, sanding should be applied⁶⁻¹⁰. The present authors¹³ predicted the maximum size of the ineffective unbonded defect area, after sanding on WRB, on peeling load using the maximum undamaged defect size concept. The details of this concept are described elsewhere¹³⁻¹⁶. Harhash et al.^{17,18} investigated the parameters on the bond strength of the roll bonded AL-ST-AL multilayers. The microstructure and mechanical properties of the Mg-Al multilayer composites fabricated to accumulative roll bonding are studies¹⁹.

In this work, the WRB process is employed to produce two different multilayer composites. The first multilayer composite is (AL/perforated CU260/AL), and the second multilayer composite is contained of five layers of (AL/PU/perforated CU260/PU/AL). The mechanical properties of such composites are investigated using a peel test and a small punch test experimentally. Moreover, the effect of the presence of pre-crack on the fracture behavior of AL/perforated CU/AL composite using a peeling test is studied numerically. Furthermore, the mechanism of the peeling test (DIN 53282) was discussed to explain the performance of specimens with different pre-crack lengths under loading conditions.

*e-mail: samousa@jazanu.edu.sa

As is already known, a small punch test (SPT) used for more than four decades to obtain mechanical properties of different materials such as tensile, fracture toughness, fatigue, and creep. European standard, Japan standard, and ASTM are doing considerable efforts to reach worldwide standardization of SPT²⁰. In the present work, it has been focused only on the applicability of SPT to determine the fracture behavior of sandwich composites. There are three patterns of SPT specimens to obtain the fracture behavior of materials, namely, smooth²¹⁻²⁴, side edge crack²⁵⁻²⁸, bottom crack²⁹⁻³². The last objective of the present work is to compare these three patterns. The validity of each cracked specimen to measure the true mode I fracture toughness is examined in the present work.

2. Materials and Experimental Procedures

The first set of the metal laminated composite was made from two Al1100 skins and one interlayer perforated copper (Cu260). Mousa and Kim^{8,9} used a fractional factorial design of experimental analysis to optimize the rolling speed and temperature for Al/PU/Al sandwich composites and they found that the optimal temperature was about 200°C and optimal rolling speed was about 30 rpm for Al/PU/Al. Based on this finding, three different combinations between the number of passes, rolling speed, and the roughness of the inner surface of AL skin were suggested in the first phase of the present work, as listed in Table 1, to show the effect of these parameters in the case of Al/perforated CU/Al sandwich composites. Preheat temperature and thickness reduction were kept constant and equal to 200°C and 60%, respectively.

The second set of experiments was carried out at the same processing parameters except adding two layers of the PU in between Al skins and interlayer perforated Cu260 as shown schematically in Figure 1. The dimensions of the Al1100, CU260, and polyurethane (PU) are (60 mm × 20 mm × 1 mm), (60 mm × 20 mm × 1.2 mm), and (60 mm × 20 mm × 0.8 mm), respectively. Table 2 summarized the mechanical properties and chemical compositions of the materials used in this study. A comparison between the two roughened AL surfaces used in the present work is shown in Figure 2.

To produce a satisfactory bond at the interface by WRB, it is essential to remove any contaminations that may be present on the surfaces of the materials to be joined. After surface preparation, samples were rolled using a laboratory rolling mill to get a reduction factor of 60%. Figure 3 shows the cross-section images of AL/perforated CU/AL and AL/PU/perforated CU/PU/AL sandwich composites. There is an interlock between two skin layers and perforated interlayer in the case of AL/perforated CU/AL sandwich composite, see Figure 3a. However, in the case of AL/PU/

Table 1. The combinations between the different manufacturing parameters.

Combinations #	Roughness, Ra (μm)	Speed (rpm)	No. of Passes
I	3.75 (Grit-80)	45	1
II	5.63 (Grit-50)	45	1
III	5.63 (Grit-50)	45	3
IV	5.63 (Grit-50)	30	3
IV	5.63 (Grit-50)	30	1

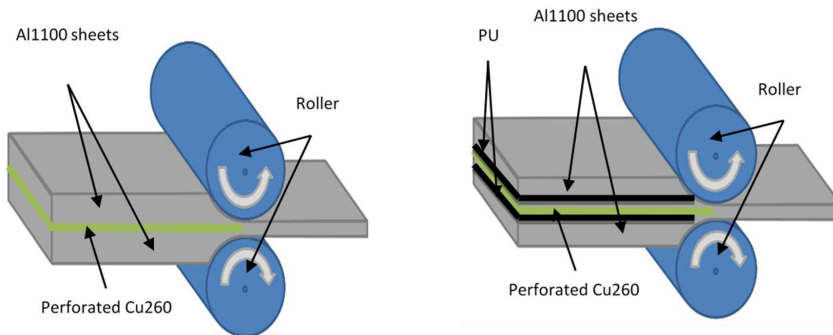


Figure 1. Schematic of manufacturing process of the Al1100/perforated CU/Al1100 multilayers composites.

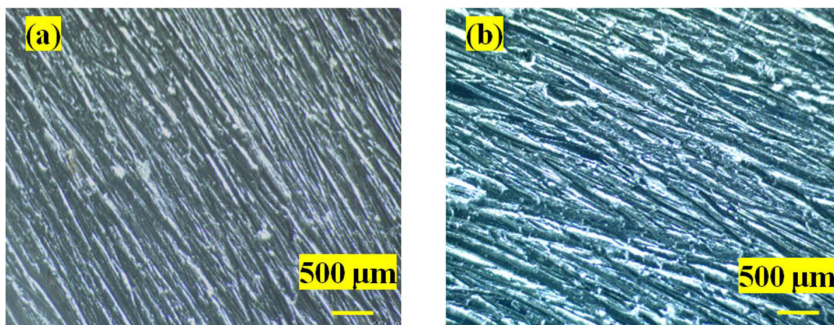
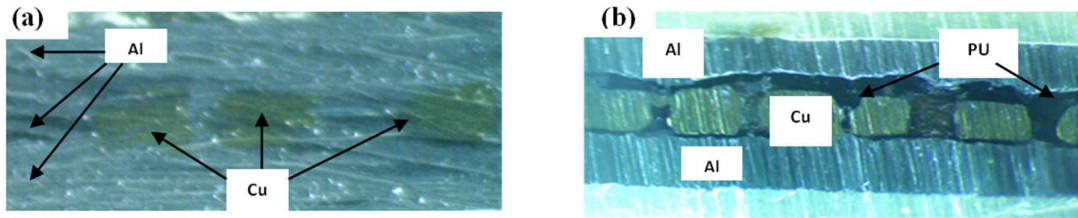
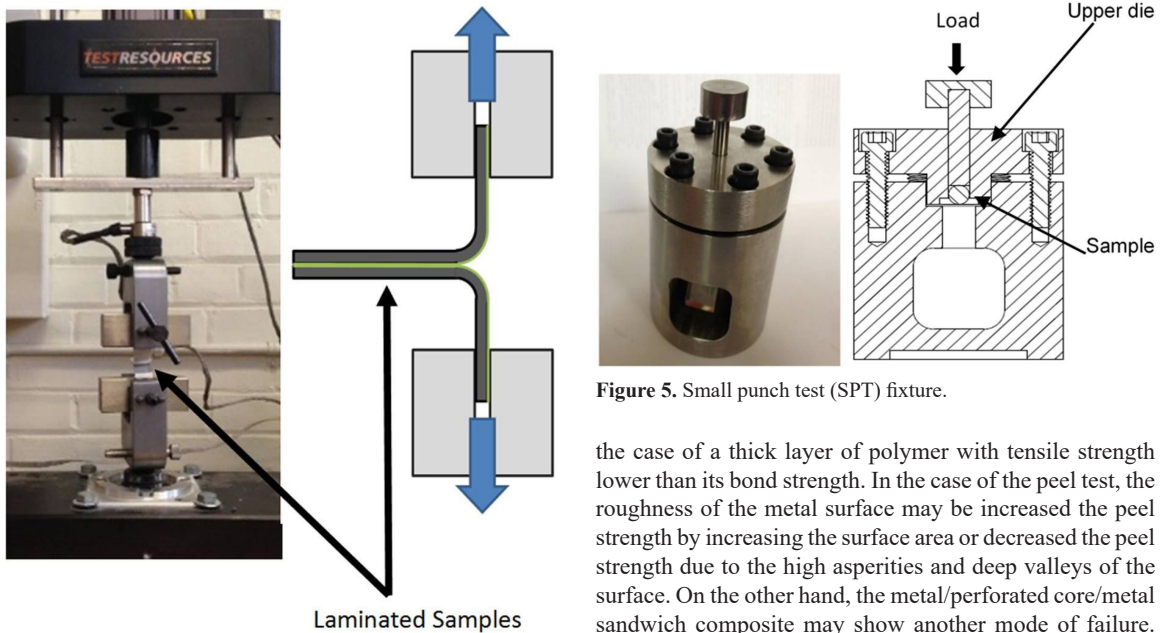


Figure 2. Optical microscopic images of the Al1100 roughened with different sandpapers grit sizes: (a) Grit-80 (Ra=3.75 μm), (b) Grit-50 (Ra=5.63 μm).

Table 2. Specification of Al1100, CU 260, and PU.

Material	Chemical composition (wt.%)	E (GPa)	ν	UTS (MPa)	Yield (MPa)	Max. Elong.%
Al1100	99.61 Al, 0.11 Si, 0.55 Fe, 0.11 Cu, and 0.07 others	75	0.33	90	34	35
CU 260	70 Cu, 0.07 Pb, 0.05 Fe, Zn balance	99	0.37	315	95	65
PU		3.6	0.45	21		300

**Figure 3.** (a) Cross section of AL/perforated CU/AL, and (b) AL/PU/perforated CU/PU/AL sandwich composites.**Figure 4.** Universal testing machine and the schematic of the peeled sample.

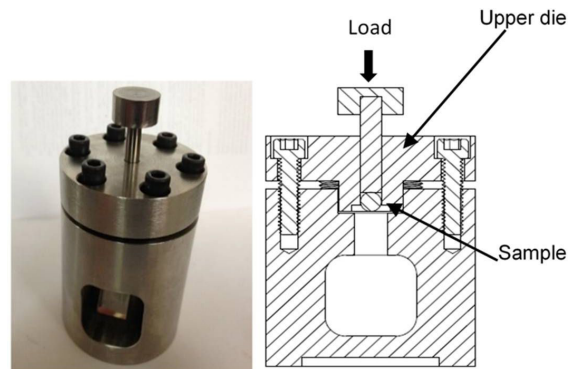
perforated CU/PU/AL sandwich composite, the interlock occurred between the PU and perforated CU.

The single lap shear test was used to determine the maximum shear load that the multilayer sample can withstand before failure occurs. The schematic and the dimensions of the sample are shown in Figure 3.

2.1. Peel test

Bond strengths between the laminated layers were measured for roll-bonded sheets using the peel test according to the ASTM D903-93 standard. In this test, the breaking-off forces were measured as shown in Figure 4, and the average peel strengths are calculated. The universal testing machine (Test Resources Inc.) was used for the testing.

In the case of metal/polymer/metal sandwich composite, the failure mode of peel test specimens may be the adhesive failure in the case of a thin layer of polymer with tensile strength higher than its bond strength or cohesive failure in

**Figure 5.** Small punch test (SPT) fixture.

the case of a thick layer of polymer with tensile strength lower than its bond strength. In the case of the peel test, the roughness of the metal surface may be increased the peel strength by increasing the surface area or decreased the peel strength due to the high asperities and deep valleys of the surface. On the other hand, the metal/perforated core/metal sandwich composite may show another mode of failure. One of the main objectives of the present study is to explore this phenomenon.

2.2. Small punch test

The small punch tests were carried out using an experimental device like the one shown in Figure 5, custom/ designed and manufactured in our laboratory, which was mounted on a universal testing machine (Test Resources Inc.) fitted with a 5 kN load cell. All details about the specifications of the SPT fixture can be found in our previous studies⁸⁻¹⁰.

The main controlling parameter in any flexural test such as SPT is flexural rigidity (EI). The stresses and deformations distribution in SPT specimens are not only dependent on EI but also dependent on the case of loading and boundary conditions. From the mechanics of materials point of view, the flexural stress in a beam made of different materials is mainly affected by the thickness and the mechanical properties of each layer in addition to the applied moment (case of loading and boundary conditions), regardless the properties of interfaces between the layers. Therefore, one of the main objectives of the present study is to verify these hypotheses.

3. Experimental Results and Discussion

Figure 6 shows the load versus displacement of the AL/perforated CU260/AL sandwich composites at different processing conditions. Specimen with a rough surface (sandpaper Grit 50), and low time processing, i.e. high rolling speed (45 rpm) and one pass rolling show the highest peak peeling load compared to those of others processing conditions but without steady-state value. It is clear from Figure 6 that increasing the surface roughness from 3.75 μm (G80) to 5.63 μm (G50) increased the peak peeling load by more than 50%. In general, the sandpaper produced surfaces with high asperities and deep valleys, which directly affected the mechanical interlocking at the interface³³. The peaks and valleys of the surface enhance the bond strength due to the increase in the effective area³⁴. It can be concluded that although the interlayer is perforated, i.e. there is an interlock between two skin layers and perforated interlayer, as shown above in Figure 3, the roughness of interface plays a crucial role of peeling resistance. The same behavior with different materials selection for the peeling test was investigated by Kamali Andani et al.¹.

On the other hand, increasing the processing time either by increasing the number of paths or decreasing the rolling speed showed the harmful effect of bonding strength, i.e. decreasing the peak peeling load. However, the sandwich composites with these manufacturing conditions have a steady-

state value of peeling load. The initial preheat temperature of the sample was 200°C, and right after rolling it was around 60°C for the one pass rolling which directly affected the results of the 3 passes rolling. In the three passes samples, the samples are cold and the effect of cold hardworking is noticeable in the results as shown in Figure 6.

Figure 7 shows the load-displacement diagrams of Al/perforated CU/Al sandwich composites at different processing conditions. Specimens with high surface roughness (G50), one rolling pass, and regardless of the rolling speed, i.e. 30 and 45 rpm, gave higher ultimate load compared to other specimens. Except for the results of the specimen with 3 passes and 45 rpm, this had odd and minimum results. However, the specimen with 3 passes and 30 rpm had results comparable with the results of the other conditions. This means that the number of passes has no harmful effect on the mechanical behavior measured from SPT. In General, it can be concluded that there is no clear effect of the processing parameters on the mechanical behavior of sandwich composites measured from SPT. This means that there is a marginal effect of interface bond strength on flexural behavior. This is in agreement with the first principles of mechanics of materials.

On the other hand, a comparison between the mechanical behavior of AL/perforated CU/AL sandwich composites and that of aluminum of the same dimensions and reduction factor, i.e. 60%, is made in Figure 7. The presence of perforated CU

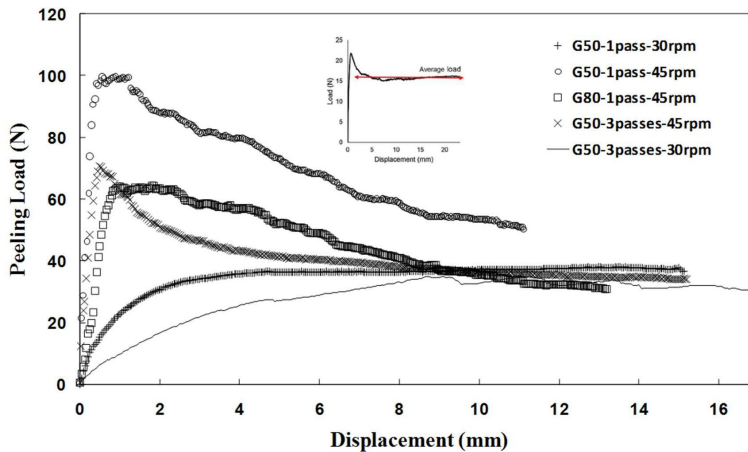


Figure 6. Load versus displacement of Al/Cu/Al sandwich composites at 200°C preheat temperature and 60% thickness reduction.

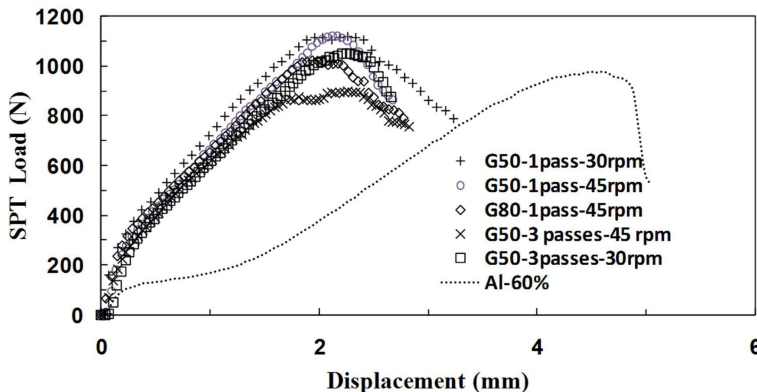


Figure 7. Experimental results of SPT specimens for different samples conditions.

around the neutral axis of the specimen has a little effect on improving the sandwich strength. However, the presence of perforated CU between the two strips of aluminum markedly improved the stiffness of the sandwich composites.

Furthermore, the relation between SPT ultimate load and the peeling load is shown in Figure 8. It is clear that there is no relation between them. This means that the SPT fails to detect the effect of processing parameters on the bond quality of WRB AL/ perforated CU/AL sandwich composites. For example, specimen with high time processing, i.e. rolling speed (30 rpm) and 3 passes rolling showed the lowest peeling resistance, see Figure 6, but it has the ultimate tensile load higher than those of lower time processing, i.e. G50-3 passes-45 rpm and G80-1 pass – 45 rpm, see Figure 7. Several researchers^{35,36} also found that the SPT is sensitive to the specimen thickness, the geometry of the test rig, and the material stress-strain response.

Figure 9 shows the peeling resistance of the 5-layers sample (AL/PU/perforated CU260/PU/AL) compared to 3-layers sample at the same conditions (rolling speed= 30 rpm, one pass, Grit-50, preheat temperature of 2000C and thickness reduction of 60%). It is clear that the presence of PU between AL skin and perforated CU decreased the bond strength of sandwich composites. This may be attributed to the interlocking strength between AL and CU is higher than that between PU and CU, see Figure 3. Figure 10 shows the peeled surface and the interlock between PU and CU. It was noticed that the separation happened at the soft layer (PU), and that can also explain the drop in the bond strength. On the other hand, the 5-layers sample reached the ultimate load of 30 N, and it can be noticed more resistance at the peak before fracture.

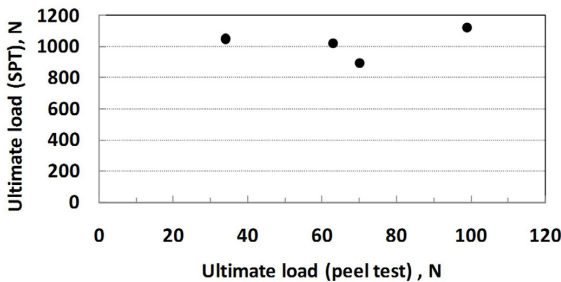


Figure 8. The relation between SPT ultimate load and the peeling load.

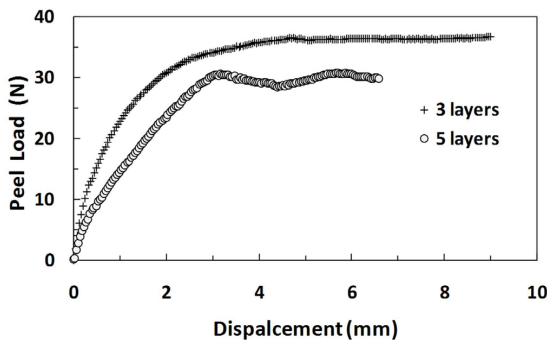


Figure 9. Load versus displacement curve for the 5 layers and 3 layers of the sandwich composites obtained from peel test (at the same rolling conditions).

The SPT specimen results of 3-layers and 5-layers samples at the same rolling conditions of the peeled samples are shown in Figure 11. The 5-layers sample reached the maximum load around 1600 N, which is improved compared to the 3-layers sample by 55%. This enhancement may be attributed to increasing the moment of inertia of the specimen.

4. Numerical Work

ABAQUS/Standard code has been utilized to simulate the peel test and SPT, as shown in Figure 12. Peel test and SPT were conducted under displacement control. In the peeling test, the crack was initiated and propagated using Virtual-Crack-Closing-Technique (VCCT) due to the crack path is known. The VCCT is used in the present work to release the bonding between the Al-Br-Al sandwich composites under peeling test based on the fracture mechanics criterion³⁷. However, an extended finite element technique was adopted in SPT to predict the crack path. The XFEM can be used to predict the crack path without remeshing and it does not need to know the crack-initiation site and the crack path like the virtual crack closure technique (VCCT)^{38,39}. Meshes of linear 8-node hexahedral brick elements (C3D8R) were generated to simulate the specimen geometries. The element type, material modeling, loading sequence, boundary conditions, and mesh sensitivity, are described elsewhere by the authors Mousa et al.¹³.

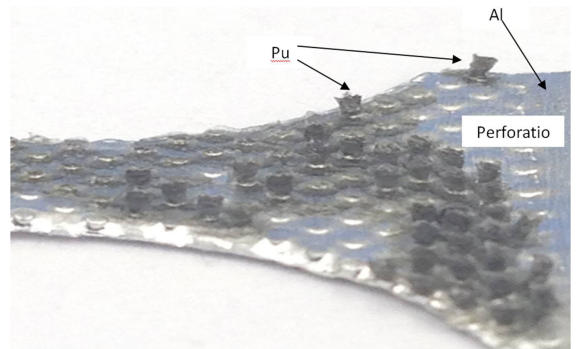


Figure 10. Peeled surface in AL/PU/perforated CU/PU/AL sandwich composite.

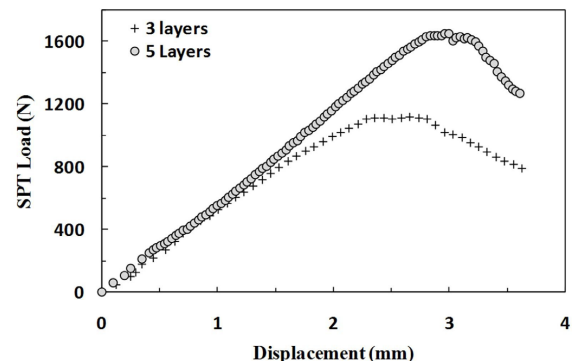


Figure 11. Load versus displacement curve for the 5 and 3 layers samples obtained from SPT (at the same rolling conditions).

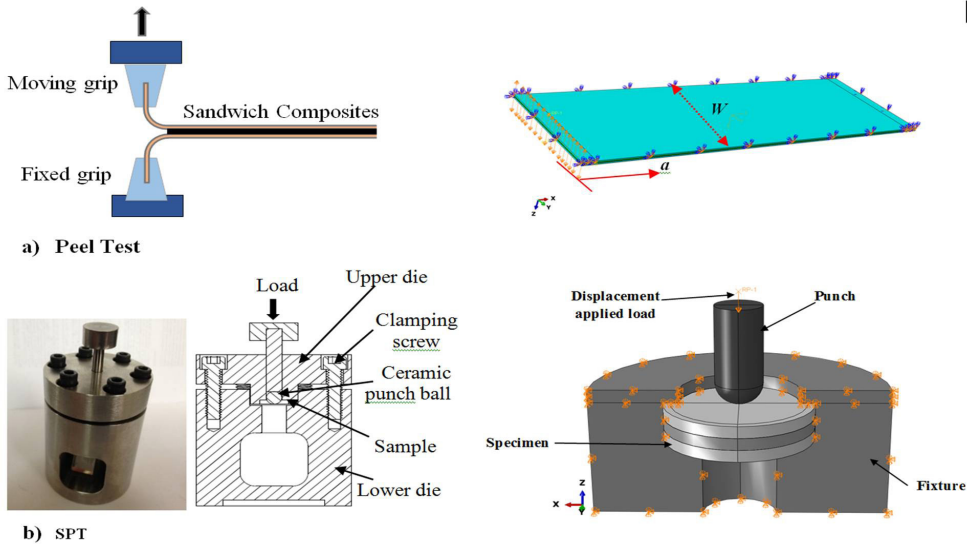


Figure 12. a) Peel test, and b) SPT setup, specimens, and idolizations.

5. Numerical Results and Discussion

5.1. Results of peeling test

To understand the mechanism of the peeling test, specimens with different crack lengths have been examined numerically. As unexpected, the descending parts of the curves did not follow/coincide with each other. This means that the stiffness of specimens having crack to width ratio equals 0.1, $a/W = 0.1$, depends on the initial crack length, i.e. compare the three curves ($a/W = 0, 0.05, \text{ and } 0.1$) in Figure 13. To understand this observation the horizontal movement of the specimen with respect to the axe of the loading was traced in the ascending and the descending parts of the curve as shown in Figure 14. It is clear that the actual crack length (distance between the crack front and the axis of the applied load) is lower than the peeling length (distance between the edge of the specimen and the crack front) due to the horizontal movement of the core of the specimen, as shown in Figure 15a. Figure 15b shows this effect of the development of the normalized mode I stress intensity factor (SIF), i.e. the geometry correction factor $f(a/W)$. It is clear that at a certain value of (a/W), ($a/W = 0.1$), the slope of the curve decreased. It can be concluded that the mechanism of the peeling test for sandwich composites contained more than two layers is different from the two-layer composites due to the horizontal movement of the interlayer.

5.2. Results of SPT

To verify the effect of interface conditions on the flexural strength of sandwich composites measured from SPT specimens, two extremes conditions, i.e. perfect bond and unbounded conditions, have been examined numerically. It is found that there is a marginal effect of interface conditions on the flexural strength of sandwich composites, as shown in Figure 16 especially if it is no clearance distance between the upper specimen surface and the lower surface of the fixture⁴⁰.

Figure 17 shows the comparison between the observed fracture surface of pure AL specimen and that predicted

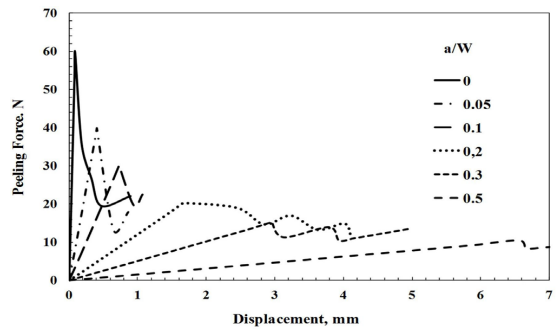


Figure 13. Effect of pre-crack on Al/CU/Al sandwich composites under peeling test.

from the FE simulation. There is a good agreement between them. The fracture may occur directly without any arresting or deviation since the specimen is made of one bulk layer. Multilayer composites may help to deviate and subsequently delay or arrest the crack.

To examine the applicability of the pre-cracked SPT specimen for determining the fracture toughness of the materials, the stress distribution around the notch root of three different notch geometries is analyzed, as shown in Figure 18. As expected the stress distribution through the SPT specimen is dependent on the curvature of the loading ball and follows Cylindrical coordinates rather than Cartesian coordinates. It is clear that the distribution of the normal stresses is not uniform near the notch root in the cases of single edge notch (SEN) and straight bottom notch (SBN). Kumar et al.³² used straight bottom notch (SBN) in plate samples to determine the crack initiation fracture toughness. They founded that the maximum stress located beside the SPT specimen furthermore the stress and strain distribution around the notch root is not uniform, that confirm with the present results.

Furthermore, the upper have of SEN surface is subjected to compressive stress. In the case of the circular bottom notch (CBN), the three normal stresses, σ_{rr} , $\sigma_{\theta\theta}$

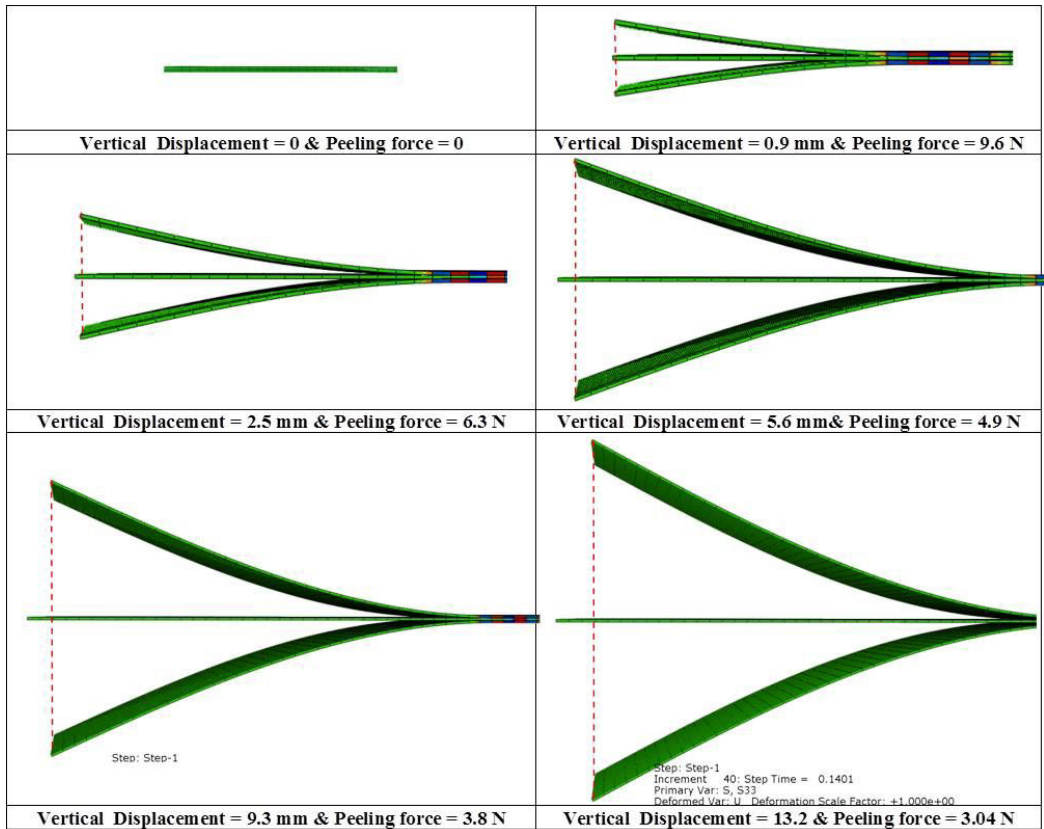


Figure 14. Horizontal movement of the specimen with respect to the axe of the loading.

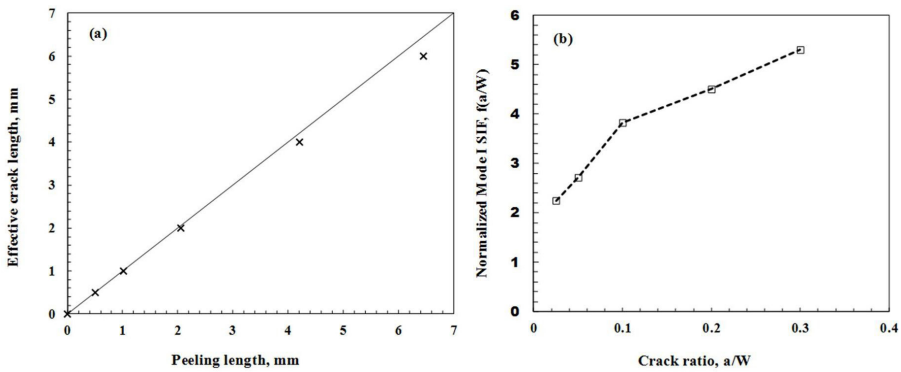


Figure 15. (a) Relation between effective crack length and peeling length, and (b) normalized mode I SIF.

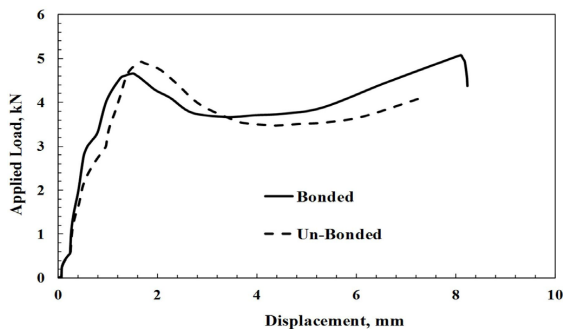


Figure 16. Effect of interface conditions on the flexural strength of sandwich composites measured from SPT specimens.

and σ_{zz} are uniformly distributed around the notch root. Therefore, CBN is a suitable geometry to steady and uniform crack growth. To study the notch sensitivity of the three different notch geometries, XFEM was adopted to predict the site of crack initiation and the path of the crack growth for smooth and pre-cracked specimens, as shown in Figures 19-21. Figure 19 shows the site of crack initiation and the path of a growing crack in SEN specimen with notch depth to specimen diameter ranged from 0 (smooth specimen) to $a/D = 0.6$. For a/D lower than 0.4, the notch insensitivity was observed. However, for a/D ranged from 0.4 to 0.6 the crack emanated from the notch root, but there are other cracks emanated from the

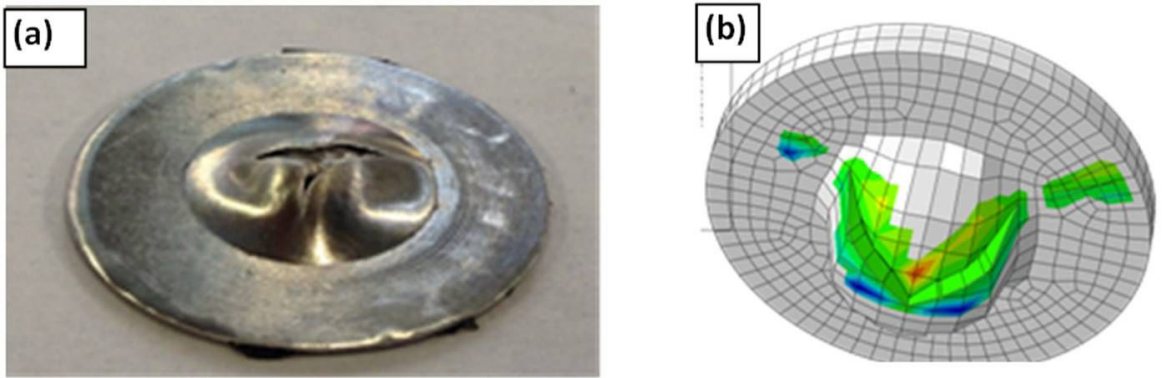


Figure 17. Al sheets after fracture in SPT, (a) experimental and (b) numerical.

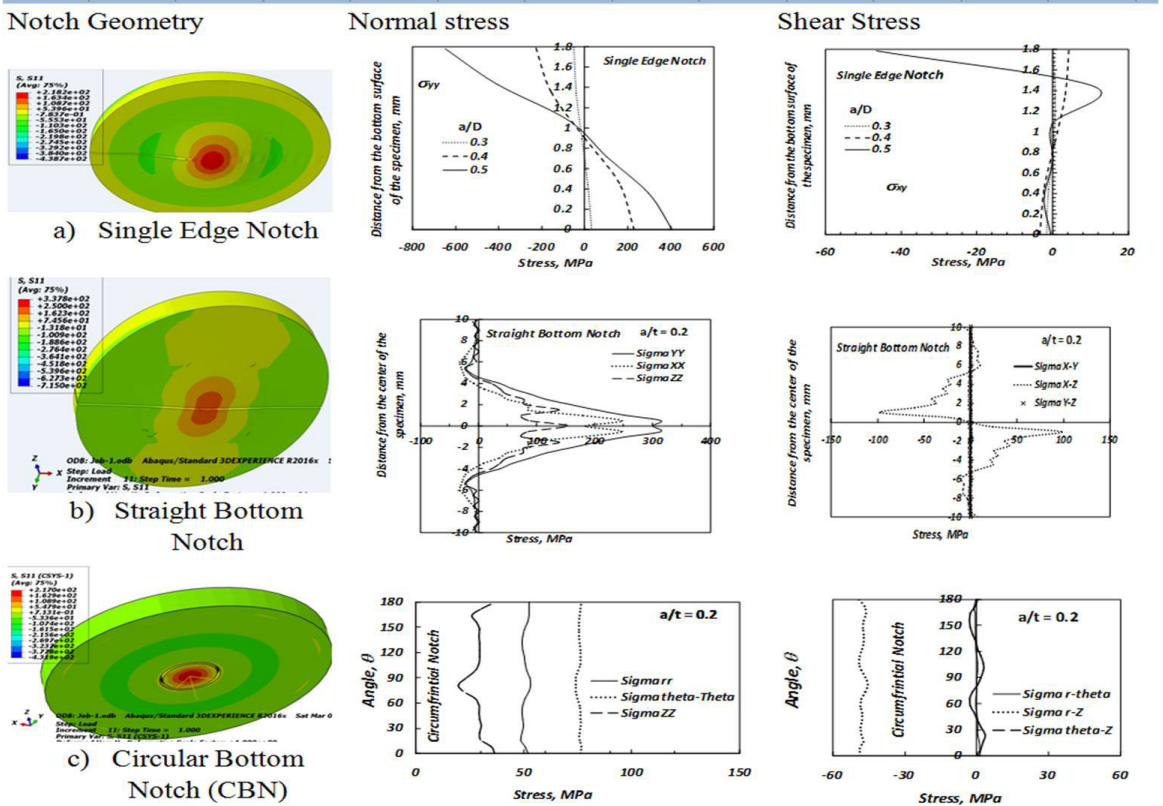


Figure 18. The stress distribution around the crack front of three different crack geometries.

smooth surface near the notch root as shown in Figure 19, that is in agreement with the Shikalgar et al.⁴¹. Wherein Shikalgar et al.⁴¹ used the pre-cracked small punch with single edge notch (SEN) to determine the fracture properties of crack like crack path, *j*-integral and crack tip opening displacement (CTOD). It is worth noting that the final failure is not affected by the presence of SEN, i.e. the shape of final failure is a circular shape, as shown in Figure 17. This observation is in agreement with the finding shown in Figure 11a of Shikalgar et al.²⁷ and in Figure 15b of Martínez-Pañeda et al.³¹.

In the case of SBN specimen with notch depth to specimen thickness ratio (*a/t*) equals two, the sites of crack initiation

and the path of growing cracks are mainly depending on the central deformation of the specimen ignoring the presence of SBN, as shown in Figure 20. The photos in Figures 4 and 19 in Kumar et al.³² and Martínez-Pañeda et al.³¹ support the present conclusion.

The same observation was found for CBN specimen with *a/t*=0.2, see Figure 21a. By increasing *a/t* to 0.5 the crack emanated from the notch root. It can be concluded that the sensitivity of CBN is dependent on *a/t* and the ratio of the circumferential of the circular notch to that of the loading ball. In general, the failure mode of the pre-cracked SPT specimen is a typical failure of a smooth SPT specimen regardless of the crack geometry.

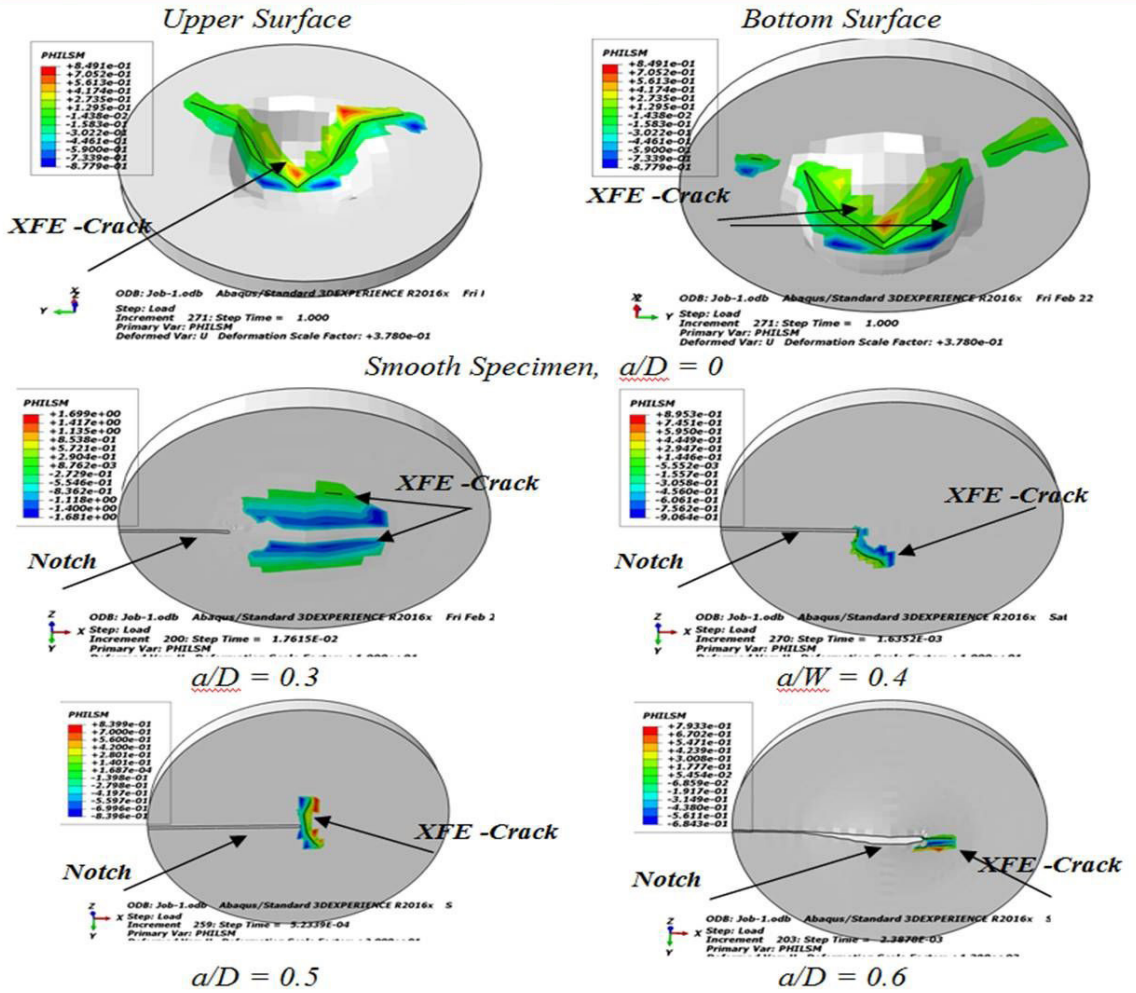


Figure 19. Site of crack initiation and crack path based on XFEM of SEN specimen.

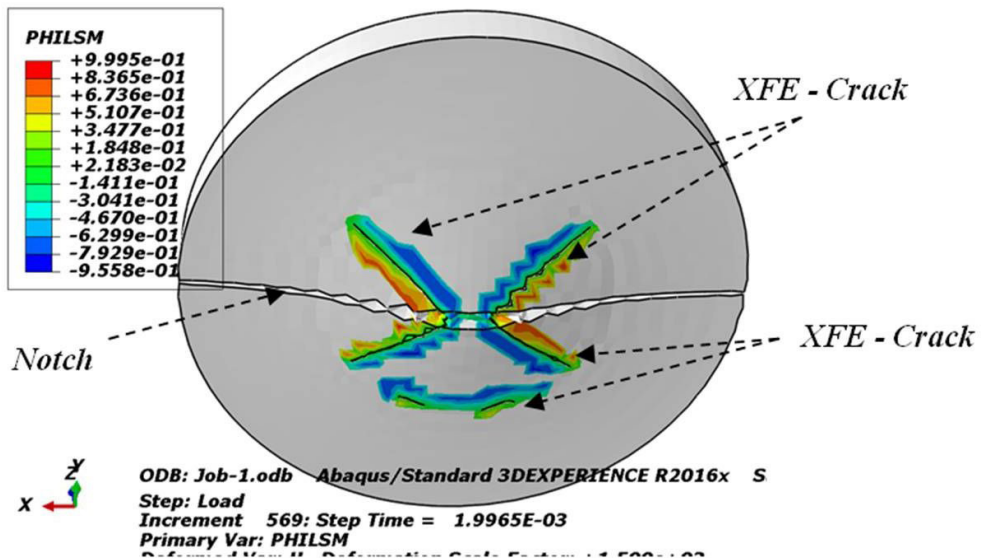


Figure 20. Site of crack initiation and crack path of SBN specimen with $a/t = 0.2$.

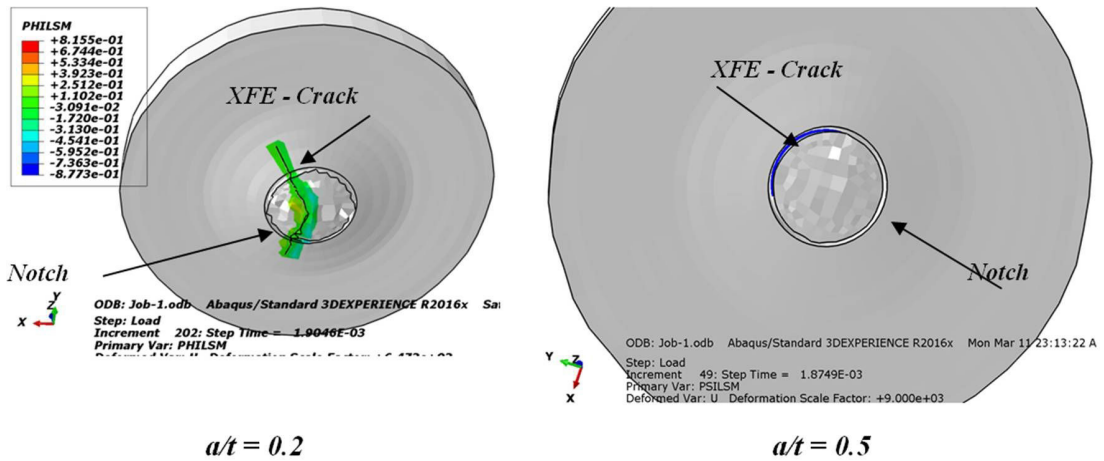


Figure 21. Site of crack initiation and crack path of CBN specimen with $a/t = 0.2$ and 0.5 .

6. Conclusions

Based on the experimental and numerical results, it can be concluded that the warm roll bonding process is a promising technique to produce multilayer composites (three layers and five layers) with different materials of combinations. The mechanism of the peeling test for sandwich composites contained more than two layers is different from the two-layer composites due to the horizontal movement of the interlayer. Using the perforated core layer led to an increase in the peel strength due to the interlocking at the interface. Increasing the surface roughness increased the peeling strength. However, increasing the number of passes during the rolling led to decrease the peel strength.

The presence of the soft layers at the core may resist the crack growth in SPT specimen. Circular bottom notch specimen is a suitable candidate to determine the fracture toughness of the materials due to its position coincides with the failure location of the SPT specimen. The sensitivity of circular bottom notch is dependent on a/t and the ratio of the circumferential of the circular notch to that of the loading ball.

7. Acknowledgments

This research was supported by the Deanship of Scientific Research (DSR) at Jazan University, Saudi Arabia. Project: DSR # waed-41-28.

8. References

- Kamali Andani M, Daneshmanesh H, Jenabali Jahromi SA. Investigation of the bonding strength of the stainless steel 316L/polyurethane/stainless steel 316L tri-layer composite produced by the warm rolling process. *J Sandw Struct Mater.* 2020;22(3):728-42.
- Stolbchenko M, Makeieva H, Grydin O, Frolov Y, Schaper M. Strain parameters at hot rolling aluminum strips reinforced with steel netting. *J Sandw Struct Mater.* 2020;22(6):2009-29.
- Tseng H-C, Hung C, Huang C-C. An analysis of the formability of aluminum/copper clad metals with different thicknesses by the finite element method and experiment. *Int J Adv Manuf Technol.* 2010;49(9-12):1029-36.
- Heness G, Wuhler R, Yeung WY. Interfacial strength development of roll-bonded aluminium/copper metal laminates. *Mater Sci Eng.* 2008;483-484:740-2.
- Abbasi M, Toroghinejad MR. Effects of processing parameters on the bond strength of Cu/Cu roll-bonded strips. *J Mater Process Technol.* 2010;210(3):560-3.
- Li L, Nagai K, Yin F. Progress in cold roll bonding of metals. *Sci Technol Adv Mater.* 2008;9(2):023001.
- Soltan Ali Nezhad M, Haerian Ardakani A. A study of joint quality of aluminum and low carbon steel strips by warm rolling. *Mater Des.* 2009;30(4):1103-9.
- Mousa S, Kim G-Y. Experimental study on warm roll bonding of metal/polymer/metal multilayer composites. *J Mater Process Technol.* 2015;222:84-90.
- Mousa S, Kim G-Y. A direct adhesion of metal-polymer-metal sandwich composites by warm roll bonding. *J Mater Process Technol.* 2017;239:133-9.
- Mousa S, Scheirer N, Kim G-Y. Roll-bonding of metal-polymer-metal sandwich composites reinforced by glass whiskers at the interface. *J Mater Process Technol.* 2018;255:463-9.
- Madaah-Hosseini HR, Kokabi AH. Cold roll bonding of 5754-aluminum strips. *Mater Sci Eng A.* 2002;335(1-2):186-90.
- Yahiro A, Masui T, Yoshida T, Doi D. Development of nonferrous clad plate and sheet by warm rolling with different temperature of materials. *ISIJ Int.* 1991;31(6):647-54.
- Mousa S, Abd-Elhady AA, Kim G-Y, Sallam HEM. Fracture behavior of roll bonded Al-brass-Al multilayer composites: concept of the maximum undamaged defect size (dmax). *Structural Integrity Procedia.* 2018;13:686-93.
- Sallam HEM, Mubarak M, Yusoff N. Application of the maximum undamaged defect size (dmax) concept in fiber reinforced concrete pavements. *Arab J Sci Eng.* 2014;39(12):8499-506.
- Abou El-Mal HSS, Sherbini AS, Sallam HEM. Mode II fracture toughness of hybrid FRCS. *International Journal of Concrete Structures and Materials.* 2015;9(4):475-86.
- Mubarak M, Sallam HEM. Reliability study on fracture and fatigue behavior of pavement materials using SCB specimen. *Int J Pavement Eng.* 2020;21(13):1563-75. <http://dx.doi.org/10.1080/10298436.2018.1555332>.
- Harhash M, Gilbert RR, Hartmann S, Palkowski H. Experimental characterization, analytical and numerical investigations of metal/polymer/metal sandwich composites – part 1: deep drawing. *Compos Struct.* 2018;202:1308-21.
- Harhash M, Gilbert RR, Hartmann S, Palkowski H. Experimental characterization, analytical and numerical investigations of metal/polymer/metal sandwich composites – part 2: free bending. *Compos Struct.* 2020;232:111421.

19. Chang H, Zheng MY, Xu C, Fan GD, Brokmeier HG, Wu K. Microstructure and mechanical properties of the Mg/Al multilayer fabricated by accumulative roll bonding (ARB) at ambient temperature. *Mater Sci Eng A*. 2012;543:249-56.
20. Lancaster R, Jeffs J. Determination of mechanical properties of materials by small punch and other miniature testing techniques. In: 5th International Small Sample Test Techniques Conference (SSTT) [Internet]; 2018; Swansea, Wales. Proceedings. Swansea: Swansea University; 2018 [cited 2021 Feb 28]. Available from: <http://sstt2018.com/proceedings.html>
21. Misawa T, Nagata S, Aoki N, Ishizaka J, Hamaguchi Y. Fracture toughness evaluation of fusion reactor structural steels at low temperatures by small punch tests. *J Nucl Mater*. 1989;169:225-32.
22. Ha JS, Fleury E. Small punch tests to estimate the mechanical properties of steels for steam power plant: II. Fracture toughness. *Int J Press Vessels Piping*. 1998;75(9):707-13.
23. Saucedo-Muñoz ML, Liu SC, Hashida T, Takahashi H, Nakajima H. Correlation between JIC and equivalent fracture strain determined by small-punch tests in JN1, JJ1 and JK2 austenitic stainless steels. *Cryogenics*. 2001;41(10):713-9. [http://dx.doi.org/10.1016/S0011-2275\(01\)00135-7](http://dx.doi.org/10.1016/S0011-2275(01)00135-7).
24. Kubík P, Šebek F, Petruška J, Hůlka J, Park N, Huh H. Comparative investigation of ductile fracture with 316L austenitic stainless steel in small punch tests: experiments and simulations. *Theor Appl Fract Mech*. 2018;98:186-98.
25. Alegre JM, Cuesta II, Barbachano HL. Determination of the fracture properties of metallic materials using pre-cracked small punch tests. *Fatigue Fract Eng Mater Struct*. 2015;38(1):104-12.
26. Alegre JM, Lacalle R, Cuesta II, Alvarez JA. Different methodologies to obtain the fracture properties of metallic materials using pre-notched small punch test specimens. *Theor Appl Fract Mech*. 2016;86:11-8.
27. Shikalgar TD, Dutta BK, Chattopadhyay J. Assessment of fracture resistance data using p-SPT specimens. *Theor Appl Fract Mech*. 2018;98:167-77.
28. Uppalancha S, Chattopadhyay J. Development of new η pl, β and limit load equations to evaluate fracture parameters of pre-cracked small punch test specimens. *Eng Fract Mech*. 2018;195:80-91.
29. Cuesta II, Willig A, Díaz A, Martínez-Pañeda E, Alegre JM. Pre-notched dog bone small punch specimens for the estimation of fracture properties. *Eng Fail Anal*. 2019;96:236-40.
30. Cárdenas E, Belzunce FJ, Rodríguez C, Penuelas I, Betegon C. Application of the small punch test to determine the fracture toughness of metallic materials. *Fatigue Fract Eng Mater Struct*. 2012;35(5):441-50.
31. Martínez-Pañeda E, García TE, Rodríguez C. Fracture toughness characterization through notched small punch test specimens. *Mater Sci Eng A*. 2016;657:422-30.
32. Kumar P, Dutta BK, Chattopadhyay J. Fracture toughness prediction of reactor grade materials using pre-notched small punch test specimens. *J Nucl Mater*. 2017;495:351-62.
33. Ekici B, Altıntaş S. Surface modification for improving the formability of SPA laminated composite. *Adv Eng Softw*. 1999;30(7):451-8.
34. Lesuer DR, Syn CK, Sherby OD, Wadsworth J, Lewandowski JJ, Hunt WH. Mechanical behaviour of laminated metal composites. *Int Mater Rev*. 1996;41(5):169-97.
35. Bruchhausen M, Holmström S, Simonovski I, Austin T, Lapetite JM, Ripplinger S, et al. Recent developments in small punch testing: tensile properties and DBTT. *Theor Appl Fract Mech*. 2016;86:2-10.
36. Garcia TE, Rodríguez C, Belzunce FJ, Suárez C. Estimation of the mechanical properties of metallic materials by means of the small punch test. *J Alloys Compd*. 2014;582:708-17.
37. Abd-Elhady AA, Mubarak MA, Sallam HEM. Progressive failure prediction of pinned joint in quasi-isotropic laminates used in pipelines. *Lat Am J Solids Struct*. 2018;15(6):e96. <http://dx.doi.org/10.1590/1679-78255061>.
38. Abd-Elhady AA, Sallam HE-DM, Mubarak MA. Failure analysis of composite repaired pipelines with an inclined crack under static internal pressure. *Procedia Structural Integrity J*. 2017;5:123-30. <http://dx.doi.org/10.1016/j.prostr.2017.07.077>.
39. Abd-Elhady AA, Sallam HE-DM, Alarif IM, Malik RA, EL-Bagory TMAA. Investigation of fatigue crack propagation in steel pipeline repaired by glass fiber reinforced polymer. *Compos Struct*. 2020;242:112189. <http://dx.doi.org/10.1016/j.compstruct.2020.112189>.
40. Mousa S, Sallam HEM, Kim AA, Abd-Elhady G-Y. Investigation on integrity assessment tests of WRB metal-polymer-metal composites. *Arch Civ Mech Eng*. 2021;21(2):60. <http://dx.doi.org/10.1007/s43452-021-00216-4>.
41. Shikalgar TD, Dutta BK, Chattopadhyay J. Assessment of fracture resistance data using p-SPT specimens. *Theor Appl Fract Mech*. 2018;98:167-77.